

Electronic Supplementary Information

Spray-drying Assembly of 3D N, P-Co-doped Graphene Microspheres Entrenched with Core-Shell CoP/MoP@C Nanoparticles for Enhanced Lithium-Ion Storage

Muhammad Ishaq, Maher Jabeen, Peiran Wang, Yu-Shi He,* Xiao-Zhen Liao, and Zi-Feng Ma

Shanghai Electrochemical Energy Devices Research Centre, School of Chemistry and Chemical Engineering, Shanghai Jiao Tong University, Shanghai 200240, China. E-mail: [ys-
he@sjtu.edu.cn](mailto:ys-he@sjtu.edu.cn)

Table S1. Summary of synthesis routes for metal phosphides.

Direct agents	Phosphorus (P)	Metal Precursors	Methods	Ref.
	Precursors			
Pure Phosphorus (P)	White Phosphorus	Metal particles	Ball milling	^{1, 2}
	Red Phosphorus		Calcination	³
	Black Phosphorus		Hydrothermal (red P)	⁴
			Solvothermal (red P)	⁵
Metallo-organic compounds	Trioctylphosphine (TOP)	Organometallic Particle	Calcination	^{6, 7}
	Tritylphosphine oxide (TOPO)			⁸
	Trimethylsilylphosphine (TMSP)			⁹
	Tributylphosphine (TBP)		Solvothermal reaction	¹⁰
	Triphenylphosphine (TPP)			¹¹
PH₃ gas	P ₄	Metal oxides	Hydrothermal reaction	^{12, 13}
	H ₂ PO ₂ ⁻	Metal halides	Temperature program reduction	^{14, 15}
	PO ₃ ³⁻	Metal phosphates		¹⁶
	PO ₄ ³	Metal phosphites	Decomposition of H ₂ PO ₂ ⁻	¹⁷
P³⁻ and others	Na ₃ P	Metallic compounds	Calcination	¹⁸
	Ca ₃ P ₂		Electrolysis	^{19, 20}
	Etc.		Solvothermal reaction	²¹

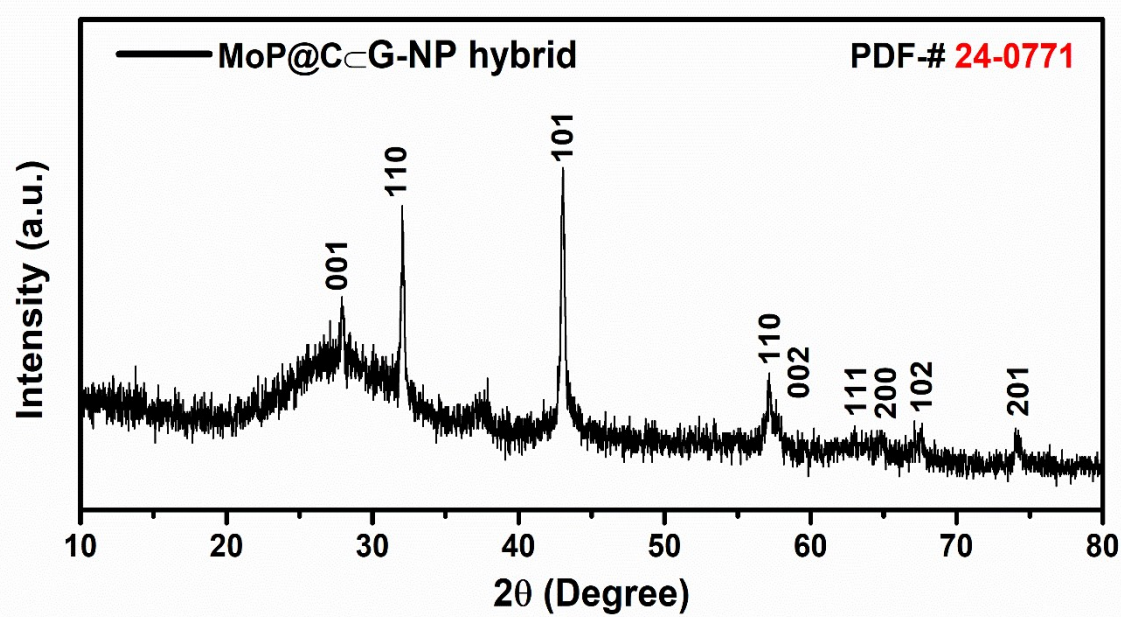


Figure S1. X-ray diffraction pattern of the as-fabricated MoP@C_nG-NP composite.

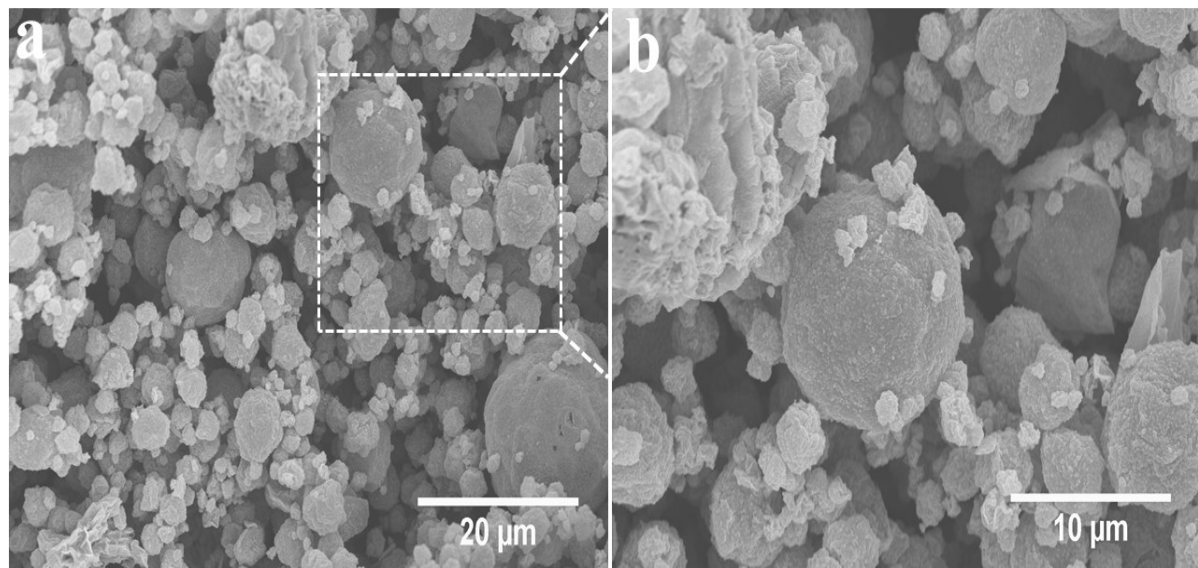


Figure S2. (a-b) SEM images of CoP@C<G-NP composit.

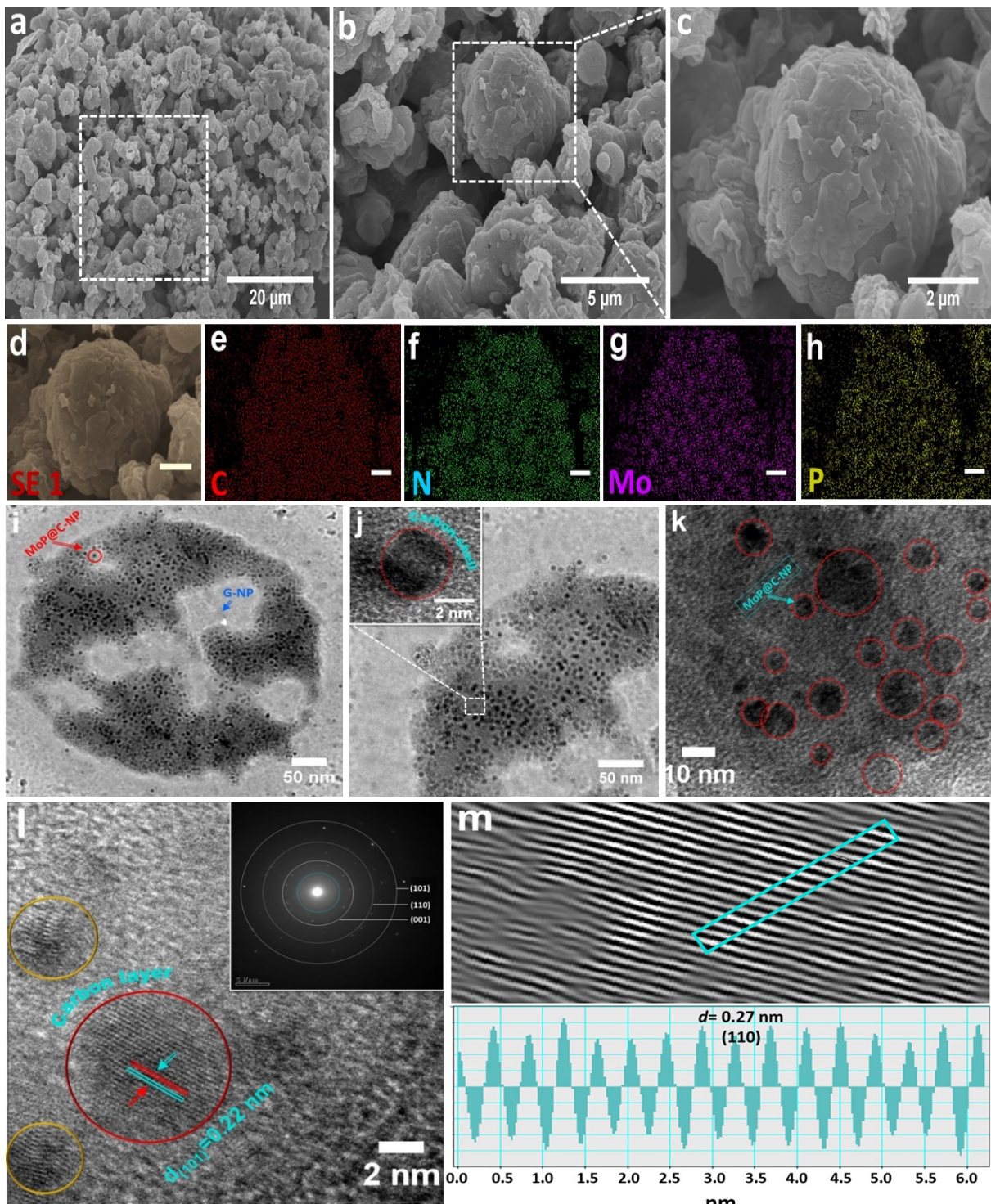


Figure S3. Structure analysis of MoP@C-NP<G-NP. (a-c) Low- and high-resolution SEM images of MoP@C<G-NP hybrid; (d-h) corresponding SEM EDS elemental mapping. Scale bar: 0.5 um. (i-k) Low-resolution TEM images and (l) high- resolution TEM lattice images show the marked d-spacing of 0.27 nm corresponding to the (110) plane of MoP@C<G-NP hybrid (Inset show selected area electron diffraction patterns), (m) and the corresponding lattices masked by Gatan Software 2.11.

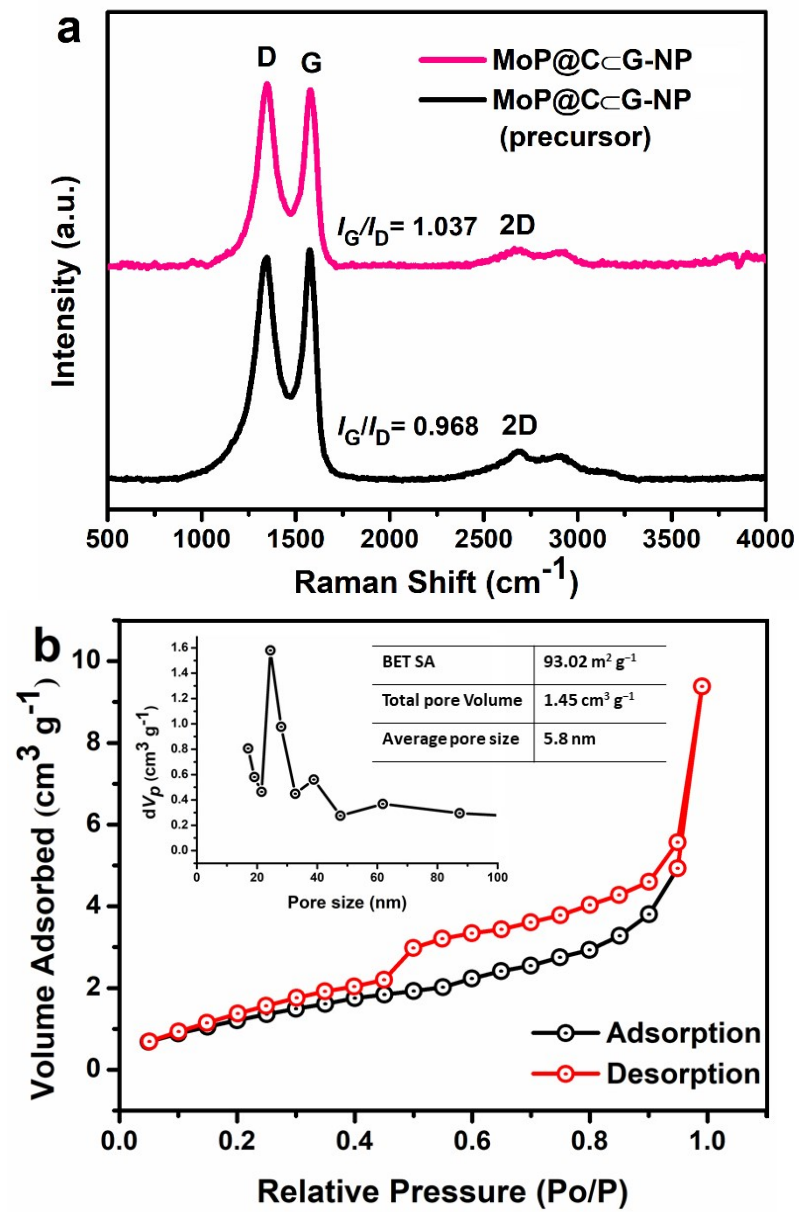


Figure S4 Chemical composition characterization of MoP@C_<G-NP composite.
 (a) Raman spectrum (b) N₂ adsorption/desorption isotherm. The inset in (b) is the corresponding pore size distribution.

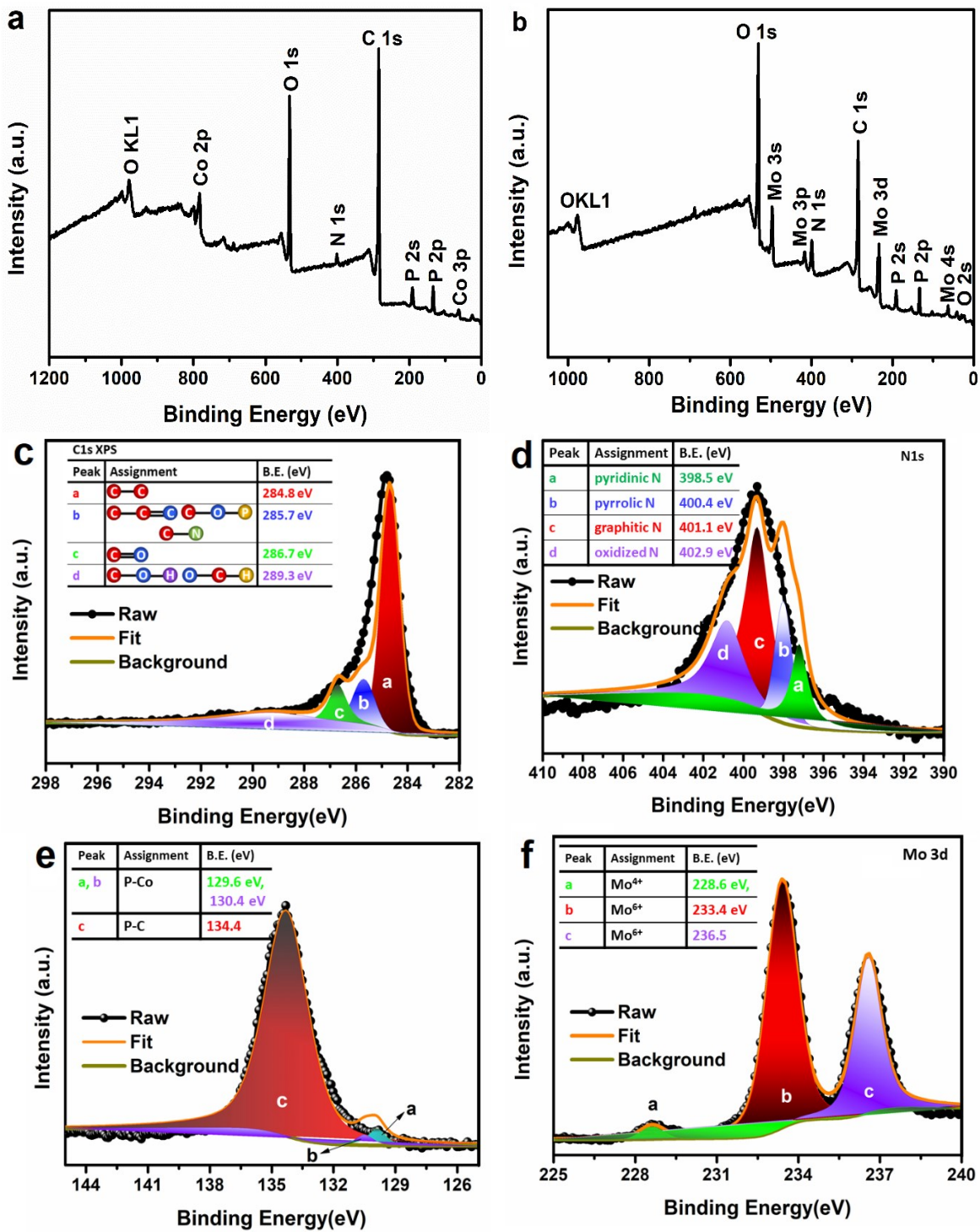


Figure S5. (a) XPS survey spectrum of CoP@C<G-NP composite. (b-f) XPS characterization of MoP@C<G-NP hybrid. (b) survey spectrum (c) high-resolution C 1s, (d) N 1s (e) P 2p, and (f) Mo 3d, respectively.

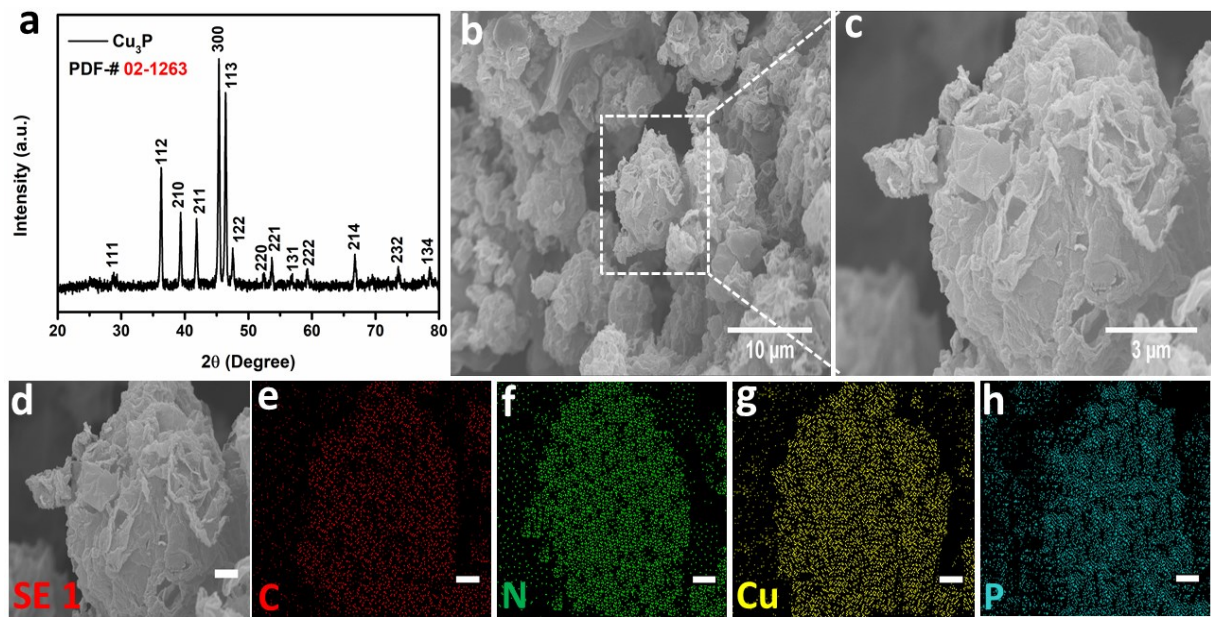


Figure S6. Structure analysis of CuP@C<G-NP. (a) XRD patterns of the CuP@C<G-NP hybrid; (b-c) Low- and high-resolution SEM images of CuP@C<G-NP hybrid; (d-h) SEM images and the corresponding elemental mapping images.

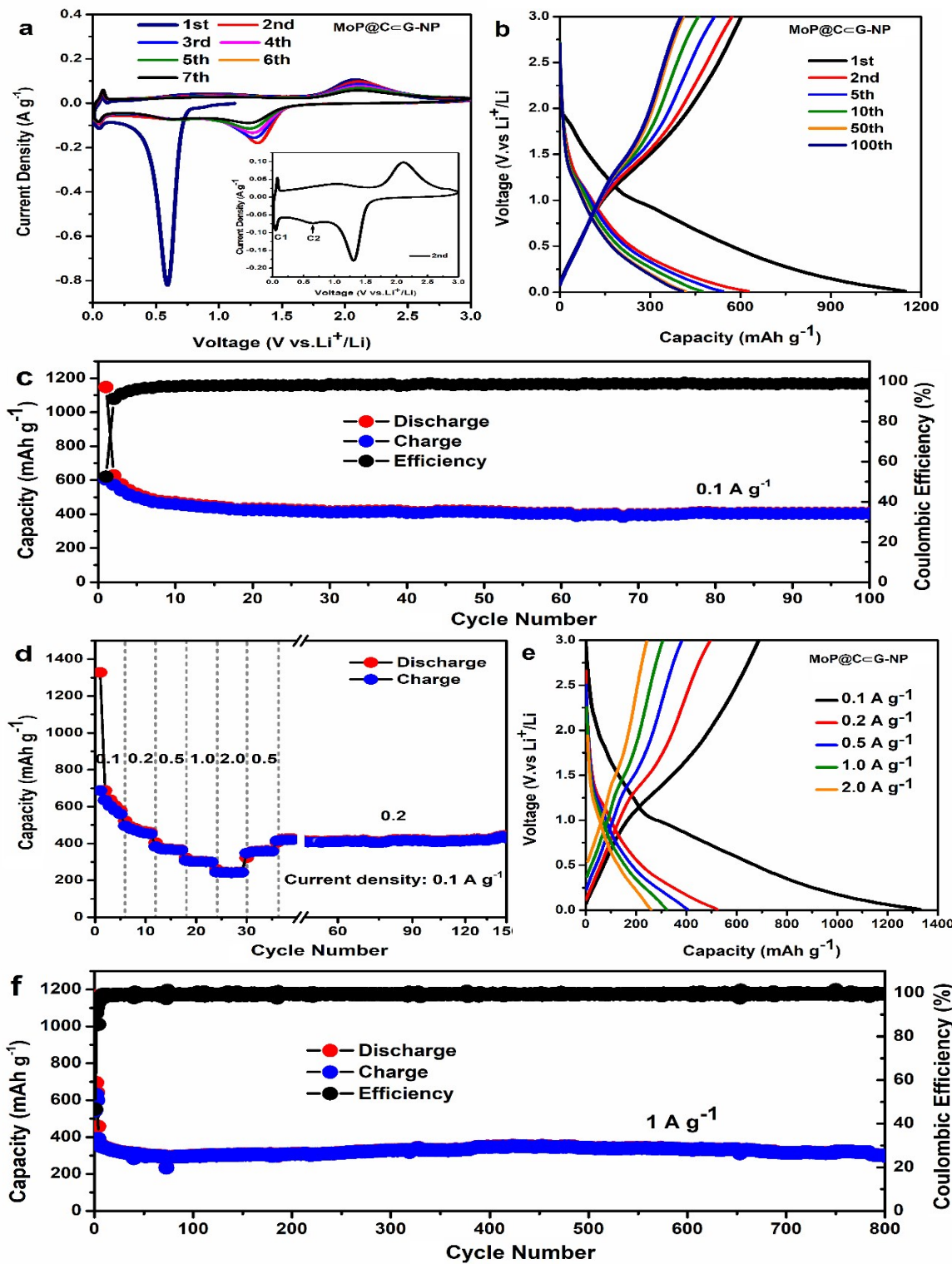


Figure S7. Electrochemical performance of the MoP@C<G-NP composite for lithium storage. (a) Cyclic voltammograms of the first seven cycles at scan rate of 0.1 mV s^{-1} . (b) Galvanostatic discharge-charge profiles. Voltage range: $0.01\text{-}3\text{V}$ versus Li^+/Li ; current density 0.1 A g^{-1} . (c) Cycling performance and the corresponding CE at 0.1 A g^{-1} . (d) Rate performance and (e) corresponding discharge-charge profiles with rates ranging from 0.1 to 2.0 A g^{-1} . (f) Long cycling performance at 1.0 A g^{-1} after 800 cycles.

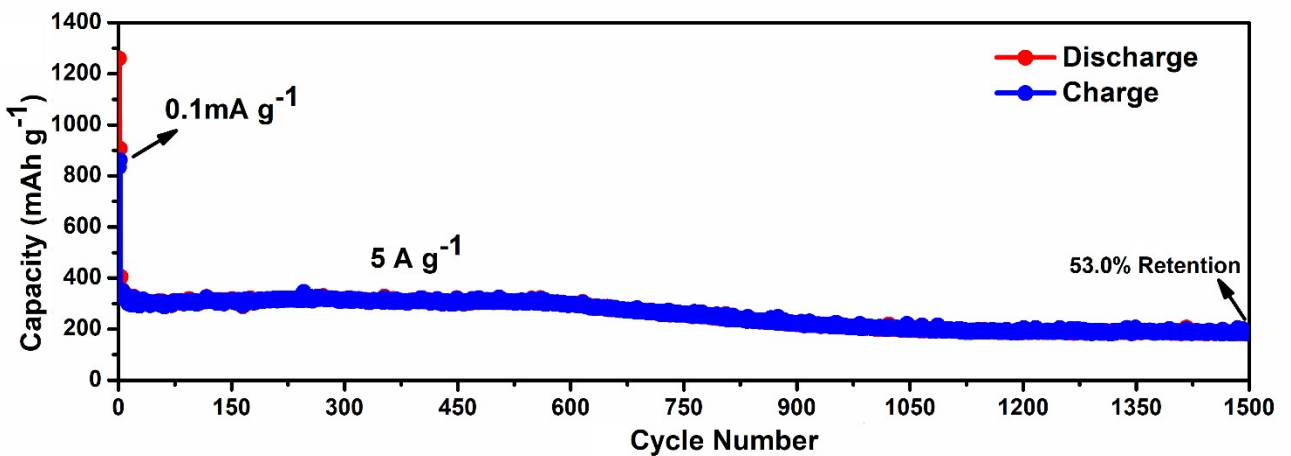


Figure S8. Long-term cycling performance of CoP@C_nG-NP electrode at a current density of 5 A g⁻¹ after 1500 cycles.

Table S2. Comparison of Li-ion storage performance of CoP@C \subset G-NP and MoP@C \subset G-NP composites with other Co/Mo phosphide composites.

Name of Electrode	Synthesis route	Capacity after cycling	Capacity retention	Ref.
CoP@C \subset PCF/NCNTs	vapor-phase phosphorization strategy	577 mAh g $^{-1}$ after 140 cycles at 0.2 A g $^{-1}$	98% after 140 cycles	²²
CoP@RGO	hydrothermal method	967 mAh g $^{-1}$ after 200 cycles at 0.2 A g $^{-1}$	83% after 200 cycles	²³
Co _x P@NC hybrid	template directing method	526 mAh g $^{-1}$ after 600 cycles at 1.0 A g $^{-1}$	78% after 600 cycles	²⁴
CoP \subset NPPCS	self-template and self-assembly strategy	437 mAh g $^{-1}$ after 800 cycles at 1 A g $^{-1}$	51% after 800 cycles	²⁵
Co-P/graphene nanocomposites	one-pot solution approach	929 mAh g $^{-1}$ after 1000 cycles at 0.1 A g $^{-1}$	83% after 100 cycles	²⁶
CoP/C nano boxes	Pyrolysis strategy	523 mAh g $^{-1}$ after 1000 cycles at 5 A g $^{-1}$	60.2 % after 1000 cycles	²⁷
Fe-CoP/CC	Hydrothermal process	1320 mAh g $^{-1}$ after 140 cycles at 0.2 A g $^{-1}$	76.5% after 200 cycles	²⁸
CoP@C-CNTs	Pyrolysis of MOFs	692 mAh g $^{-1}$ after 100 cycles at 0.1 A g $^{-1}$	81% after 100 cycles	²⁹
CoP@CNCs	Pyrolysis-phosphorization method	714.1 mAh g $^{-1}$ after 500 cycles at 2 A g $^{-1}$	77 % after 500 cycles	³⁰
CoP@NC/rGO	In situ growth of Co-MOFs	733 mAh g $^{-1}$ after 300 cycles at 0.25 A g $^{-1}$	91 % after 300 cycles	³¹
CoP@C/BC	Hydrothermal method	351 mAh g $^{-1}$ after 1000 cycles at 1 A g $^{-1}$	82.9 % after 1000 cycles	³²
CoP@N/P-(C/CNTs)	Pyrolysis-phosphorization strategy	600 mAh g $^{-1}$ after 200 cycles at 0.5 A g $^{-1}$	81.6 % after 200 cycles	³³
CoP nanorod arrays		390 mAh g $^{-1}$ after 900 cycles at 0.4 A g $^{-1}$	53% after 900 cycles	³⁴
CoP HR@rGO	Hydrothermal and phosphorization method	714.7 mAh g $^{-1}$ after 100 cycles at 0.1 A g $^{-1}$	78% after 100 cycles	³⁵
CoP/C nanosheets	Carbonization-phosphorization strategy	612 mAh g $^{-1}$ after 500 cycles at 0.4 A g $^{-1}$	77.2 % after 500 cycles	³⁶
CoP3@PPy microcubes	Template method	650 mAh g $^{-1}$ after 220 cycles at 0.5 A g $^{-1}$	81.2 % after 220 cycles	³⁷
3D porous MoP@C hybrid	Template sol-gel method	1028 mAh g $^{-1}$ after 100 cycles at 0.1 A g $^{-1}$	83.4 % after 100 cycles	³⁸
MoP-C microspheres	Carbonization and phosphorization	1152 mAh g $^{-1}$ after 1200 cycles at 0.2 A g $^{-1}$	79.2 % after 100 cycles	³⁹
H-MoP@rGO	Hydrothermal-phosphorization method	353.8 mAh g $^{-1}$ after 600 cycles at 1 A g $^{-1}$	74.3 % after 100 cycles	⁴⁰
MoP@C	Self-polymerization-phosphidation	496 mAh g $^{-1}$ after 400 cycles at 1 A g $^{-1}$	93 % after 400 cycles	⁴¹

	strategy			
MoP@NCNFs	electrospinning method	840 mAh g ⁻¹ after 200 cycles at 0.1 A g ⁻¹	77.3 % after 200 cycles	⁴²
CoP@C \subset G-NP	Spray-drying	494 mAh g ⁻¹ after 500 cycles at 0.5 A g ⁻¹	86.7 % after 500 cycles	This work
CoP@C \subset G-NP	Spray-drying	438 mAh g ⁻¹ after 500 cycles at 1 A g ⁻¹	74.7 % after 500 cycles	This work
MoP@C \subset G-NP	Spray-drying	301 mAh g ⁻¹ after 800 cycles at 1 A g ⁻¹	87.4 % after 800 cycles	This work

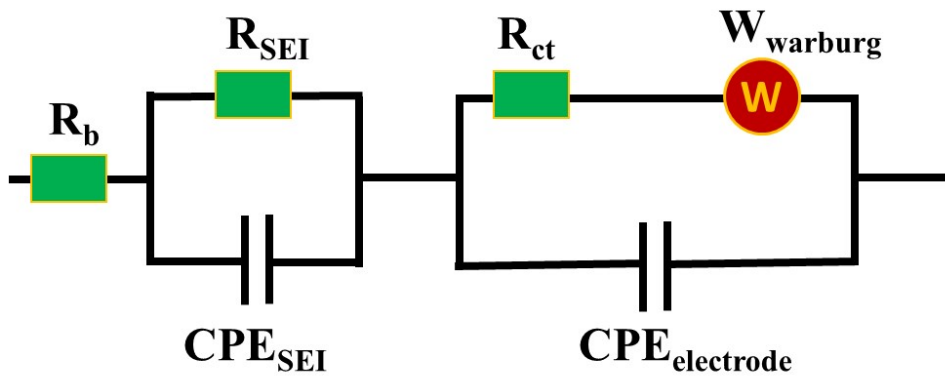


Figure S9. Equivalent circuit model used for fitting the CoP@C_xG-NP and MoP@C_xG-NP electrodes Nyquist plots in half-cell system. Where R_b: bulk resistance of cell (electrolyte, separator, and electrodes). R_{SEI}, CPE_{SEI}: resistance and capacitance of the interfacial layer. R_{ct}, CPE_{electrode}: charge-transfer resistance and double layer capacitance. W: Warburg impedance (diffusional effects of Li ion on the host material).

Table S3. EIS Fitting parameters.

CoP@C _x G-NP	R _b /Ohm	R _{SEI} /Ohm	R _{ct} /Ohm	W/Ohm
Before cycles	6.5	9.5	357.7	84.6
After 25 th cycles	17.8	11.6	77.1	46.7
After 50 th cycles	4.7	10.4	165.6	48.2
MoP@C_xG-NP				
Before cycles	9.8	10.4	334.1	83.4
After 25 th cycles	19.7	12.8	66.1	51.7
After 50 th cycles	2.8	11.4	121.4	45.1

References

1. T. L. Kulova and A. M. Skundin, *Russian Journal of Electrochemistry*, 2020, **56**, 1-17.
2. J. Sun, C. Liu and P. Yang, *Journal of the American Chemical Society*, 2011, **133**, 19306-19309.
3. X. Li, A. M. Elshahawy, C. Guan and J. Wang, *Small*, 2017, **13**, 1701530.
4. Y. Fu, Q. Wei, G. Zhang and S. Sun, *Advanced Energy Materials*, 2018, **8**, 1703058.
5. J. Liu, X. Chen, M. Shao, C. An, W. Yu and Y. Qian, *Journal of crystal growth*, 2003, **252**, 297-301.
6. Y. Pan, Y. Lin, Y. Chen, Y. Liu and C. Liu, *Journal of Materials Chemistry A*, 2016, **4**, 4745-4754.
7. M. Walter, M. I. Bodnarchuk, K. V. Kravchyk and M. V. Kovalenko, *CHIMIA International Journal for Chemistry*, 2015, **69**, 724-728.
8. C. Qian, F. Kim, L. Ma, F. Tsui, P. Yang and J. Liu, *Journal of the American Chemical Society*, 2004, **126**, 1195-1198.
9. M. Sun, H. Liu, J. Qu and J. Li, *Advanced Energy Materials*, 2016, **6**, 1600087.
10. P. Ramasamy, K.-J. Ko, J.-W. Kang and J.-S. Lee, *Chemistry of Materials*, 2018, **30**, 3643-3647.
11. T. Chouki, M. Machreki and S. Emin, *International Journal of Hydrogen Energy*, 2020, **45**, 21473-21482.
12. A. Wang, M. Qin, J. Guan, L. Wang, H. Guo, X. Li, Y. Wang, R. Prins and Y. Hu, *Angewandte Chemie International Edition*, 2008, **47**, 6052-6054.
13. L. Guo, Y. Zhao and Z. Yao, *Dalton Transactions*, 2016, **45**, 1225-1232.
14. Q. Guan and W. Li, *Journal of Catalysis*, 2010, **271**, 413-415.
15. L. Peng, S. S. A. Shah and Z. Wei, *Chinese Journal of Catalysis*, 2018, **39**, 1575-1593.
16. Y. Donghang, T. Junyan, B. Rongbiao, Y. Shuyi, J. Mengnan, K. Zigui, H. Li, F. Wang and L. Caolong, *Nanoscale Research Letters*, 2021, **16**.
17. Z. Wang, Z. Qi, X. Fan, D. Y. Leung, J. Long, Z. Zhang, T. Miao, S. Meng, S. Chen and X. Fu, *Applied Catalysis B: Environmental*, 2021, **281**, 119443.
18. C. Chang, S. Zhu, X. Liu, Y. Chen, Y. Sun, Y. Tang, P. Wan and J. Pan, *Industrial & Engineering Chemistry Research*, 2021.
19. L. Jin, X. Zhang, W. Zhao, S. Chen, Z. Shi, J. Wang, Y. Xie, F. Liang and C. Zhao, *Langmuir*, 2019, **35**, 9161-9168.
20. P. Ivan, *Journal of Materials Chemistry*, 1994, **4**, 279-283.
21. C. Wang, L. Chai, C. Luo and S. Liu, *Applied Surface Science*, 2021, **540**, 148336.
22. K. Guo, B. Xi, R. Wei, H. Li, J. Feng and S. Xiong, *Advanced Energy Materials*, 2020, **10**, 1902913.
23. J. Yang, Y. Zhang, C. Sun, H. Liu, L. Li, W. Si, W. Huang, Q. Yan and X. Dong, *Nano Research*, 2016, **9**, 612-621.
24. Y. Liu, X. Que, X. Wu, Q. Yuan, H. Wang, J. Wu, Y. Gui and W. Gan, *Materials Today Chemistry*, 2020, **17**, 100284.
25. J. Bai, B. Xi, H. Mao, Y. Lin, X. Ma, J. Feng and S. Xiong, *Advanced Materials*, 2018, **30**, 1802310.
26. Q. Xie, D. Zeng, P. Gong, J. Huang, Y. Ma, L. Wang and D.-L. Peng, *Electrochimica Acta*, 2017, **232**, 465-473.

27. X. Wang, Z. Na, D. Yin, C. Wang, Y. Wu, G. Huang and L. Wang, *ACS Nano*, 2018, **12**, 12238-12246.
28. L. Ni, G. Chen, X. Liu, J. Han, X. Xiao, N. Zhang, S. Liang, G. Qiu and R. Ma, *ACS Applied Energy Materials*, 2019, **2**, 406-412.
29. P. Zhu, Z. Zhang, P. Zhao, B. Zhang, X. Cao, J. Yu, J. Cai, Y. Huang and Z. Yang, *Carbon*, 2019, **142**, 269-277.
30. W. Li, R. Zhao, K. Zhou, C. Shen, X. Zhang, H. Wu, L. Ni, H. Yan, G. Diao and M. Chen, *Journal of Materials Chemistry A*, 2019, **7**, 8443-8450.
31. X. Zhao, D. Luo, Y. Wang and Z.-H. Liu, *Nano Research*, 2019, **12**, 2872-2880.
32. J. Jiang, K. Zhu, Y. Fang, H. Wang, K. Ye, J. Yan, G. Wang, K. Cheng, L. Zhou and D. Cao, *Journal of Colloid and Interface Science*, 2018, **530**, 579-585.
33. C. Yao, J. Xu, Y. Zhu, R. Zhang, Y. Shen and A. Xie, *Applied Surface Science*, 2020, **513**, 145777.
34. X. Xu, J. Liu, R. Hu, J. Liu, L. Ouyang and M. Zhu, *Chemistry – A European Journal*, 2017, **23**, 5198-5204.
35. Z. Han, B. Wang, X. Liu, G. Wang, H. Wang and J. Bai, *Journal of Materials Science*, 2018, **53**, 8445-8459.
36. W. Wang, J. Li, M. Bi, Y. Zhao, M. Chen and Z. Fang, *Electrochimica Acta*, 2018, **259**, 822-829.
37. Q. Liu, Y. Luo, W. Chen, Y. Yan, L. Xue and W. Zhang, *Chemical Engineering Journal*, 2018, **347**, 455-461.
38. X. Wang, P. Sun, J. Qin, J. Wang, Y. Xiao and M. Cao, *Nanoscale*, 2016, **8**, 10330-10338.
39. X. Yang, Q. Li, H. Wang, J. Feng, M. Zhang, R. Yuan and Y. Chai, *Inorganic Chemistry Frontiers*, 2018, **5**, 1432-1437.
40. Y. Yin, L. Fan, Y. Zhang, N. Liu, N. Zhang and K. Sun, *Nanoscale*, 2019, **11**, 7129-7134.
41. C. Ma, C. Deng, X. Liao, Y. He, Z. Ma and H. Xiong, *ACS Applied Energy Materials*, 2018, **1**, 7140-7145.
42. C. Fu, H. Yang, G. Feng, L. Wang and T. Liu, *Electrochimica Acta*, 2020, **358**, 136921.